

Velocity filtering using complementary gratings in photorefractive BSO

Ghazanfar Hussain and Robert W. Eason

Department of Physics and Optoelectronics Research Centre, University of Southampton, Southampton SO9 5NH, UK

Received 25 April 1991

We demonstrate a new optical technique for velocity filtering and feature extraction of time varying optical images. The technique exploits the recording of complementary (multiplexed) gratings with a relative phase shift of 180° in a photorefractive material, BSO, via a degenerate four wave mixing (DFWM) configuration. For experimental parameters, such as grating response time and optimised total input intensity, almost complete subtraction is achieved in the phase conjugate output. When motion occurs in the object plane a bright output image is observed depending on the experimental variables of feature size and velocity. We present results for motion detection of features of various dimensions at a range of speeds in both x and y directions and via Fourier plane observation.

1. Introduction

Motion detection, velocity filtering and the detection of change in a given scene are all important aspects for optical processing architectures and systems. Fields in which this capability has immediate applications include industrial inspection, bio-medical screening techniques, machine vision, and artificial intelligence techniques. So far several different techniques have been reported in the literature that use either all optical [1-4], or hybrid (optical plus electronic) [5,6], schemes to implement novelty filter [1] type operations.

A recently reported hybrid technique [5] uses an active matrix liquid crystal TV in conjunction with a position sensitive device and a TV frame memory to track a moving object within a TV image. This technique however may have only limited applications due to the sequential nature of the process and cannot easily be adapted to track more than one moving object. Another hybrid technique has used a white light source and two liquid crystal spatial light modulators in a cascaded configuration to implement optical delay [6]. Both of these techniques rely upon pixel by pixel subtraction between a previously stored (or reference) image and a second constantly updated image.

For essentially all-optical schemes the intrinsic advantages of parallel image subtraction are clear. So far several different optical techniques have been reported which rely either on phase conjugate Michelson interferometer arrangements [1,2], or alternatively two beam coupling schemes [3,4] and depend on differential response time, and transient energy transfer respectively. Apart from ref. [2], all these schemes use photorefractive BaTiO_3 , which has the drawback of a comparatively slow response time. Also for transmission devices (for the two-beam coupling schemes) distortion of the output images may occur.

In this paper we report a different scheme for motion detection and velocity filtering which uses a single object beam with a periodically phase modulated reference beam to write two spatially multiplexed gratings with a phase shift of 180 degrees. Under static conditions in the output plane the diffraction from these multiplexed gratings leads to destructive interference. In the case of motion however, an output image is seen as the former complete subtraction no longer occurs.

2. Theoretical considerations

Volume holographic gratings recorded via induced nonlinear electro-optic effects in materials such as $\text{Bi}_{12}\text{SiO}_{20}$ and $\text{Bi}_{12}\text{GeO}_{20}$ have been studied extensively for more than ten years now, and are discussed in detail in ref. [7]. Spatial multiplexing of two such gratings is also possible in these materials with an arbitrary spatial phase shift between the two gratings. For a 180° phase shift these two gratings are termed complementary and such complementary grating recording has already been implemented in a LiNbO_3 crystal [8], where sequential recording followed by continuous readout gave rise to subtraction between the two phase conjugate outputs: the "exclusive OR" operation was also demonstrated for non-identical sequential inputs.

Optical motion detection however can benefit considerably from the use of a reasonably fast material, such as photorefractive BSO. Multiplexing is also easy to achieve and four simultaneous multiplexed gratings have been recorded in BSO [9] using four different object beams forming different angles with a common reference beam. Using such angular multiplexing we have already reported a technique that uses two gratings to detect motion via DFWM in a BSO crystal [2].

Here we consider a different approach that uses complementary grating recording, in which the reference beam is subject to a periodic phase modulation. When the two gratings recorded in this way experience a relative phase shift of one half of the grating period, a subtraction in the phase conjugate output occurs.

The principle of subtraction can be described by considering the photoinduced index modulation Δn_A and Δn_B of the two volume holograms recorded for the same object beam with the 180° phase modulated reference beam. The resultant superposed index modulations are thus

$$\Delta n_A = N_A \cos[Kx + \phi_A(x)],$$

$$\Delta n_B = N_B \cos[Kx + \phi_B(x)],$$

where x is the spatial co-ordinate and K is the grating wave vector. Subtraction is realized when both multiplexed gratings are of identical strength and $\Delta n_A + \Delta n_B = 0$. Here N_A and N_B contain all the in-

formation regarding grating modulation strength etc. and ϕ_A, ϕ_B are the relative lateral phase shifts of the two gratings.

In the case of a static object these grating profiles are identical and the phase conjugate output is ideally reduced to zero. If any movement occurs in the object plane however these multiplexed gratings will undergo dynamic change and any resultant output will indicate motion within the object plane.

3. Experimental arrangements

Fig. 1 shows the details of the experimental arrangement for motion detection via this multiplexed degenerate four wave mixing configuration. An argon ion laser operating in multi-longitudinal mode at 514.5 nm was spatially filtered and expanded to a diameter of ≈ 5 mm and split by beam splitter BS_1 . The reflected beam was directed towards mirror M_2 which was mounted on a piezo-electric pusher driven by a variable frequency square wave ac voltage. M_2 reflected the incident beam towards the BSO crystal. The transmitted beam through BS_1 was split by BS_2 to form an object beam I_2 and a mutually incoherent counter propagating readout beam I_3 . Beam I_2 was incident on the BSO, after traversing an object, beam splitter BS_3 , and imaging lens L_1 ($f=15$ cm).

The intensities of the beams I_1, I_2 and I_3 were arranged to be 7.0 mW, 3.5 mW and 1.7 mW respectively. Lens L_1 was used for 1:1 imaging of the input

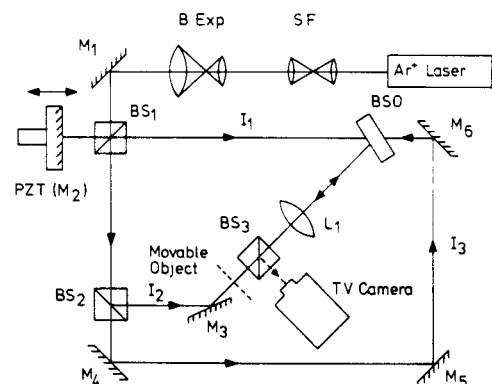


Fig. 1. The experimental arrangement for velocity filtering using complementary gratings in photorefractive BSO.

light distribution into the BSO crystal. The angle between the beams I_1 and I_2 outside the crystal was 40° . Under normal conditions (i.e., when no voltage was applied to the piezo-electric pusher) normal DFWM occurred. To write the complementary gratings a square wave ac voltage was applied to the piezo-electric pusher in the reference beam with a controllable frequency in the range of 0–100 Hz and driving voltage 0–30 V.

Fig. 2 shows the phase conjugate output, measured by a photodiode at the image plane, versus the amplitude of the square waveform ac voltage applied to the pusher for the above input laser intensities. The curve shows several minima in the output intensity which correspond to subtraction of the two outputs. At these voltage values the pusher introduces a net phase shift of π (or odd multiples of π) between the two gratings. It was observed that at higher incident laser intensities, appropriately higher frequencies of the ac waveform were required due to the shorter recording and erasing time of the multiplexed gratings. After the first maximum in the phase conjugate output, a decrease in the subsidiary intensity maxima occurs, which may be due to the erasure caused by "sweeping" of the gratings through the BSO for progressively larger ac voltages applied to the piezo-electric pusher.

The subtraction by complementary gratings can be illustrated via a model shown in fig. 3, which considers the simultaneous presence of two spatially multiplexed gratings of variable photoinduced index

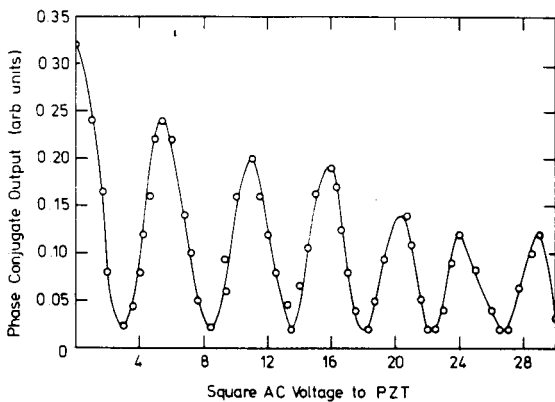


Fig. 2. Phase conjugate output from complementary gratings versus amplitude of the square waveform ac voltage applied to the piezo-electric pusher (fit to data points is visual only).

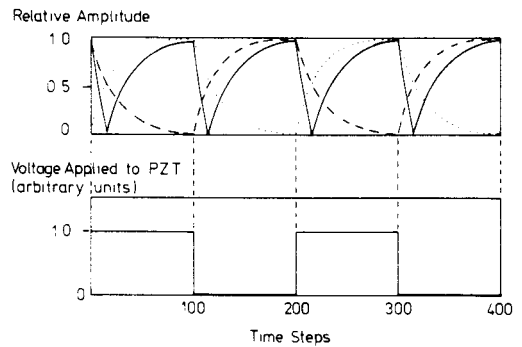


Fig. 3. Result of simulation for the complementary gratings build up, decay, and the differential output. Dotted and dashed lines indicate decay and growth of the two gratings respectively. The solid line indicates differential output.

modulation. For this simulation both curves (dashed and dotted lines) have a single exponential decay and growth constant during each of the 100 time step intervals. For this case we have assumed that the decay and growth time constants τ_1 and τ_2 are not equal, and have set them at 25 and 20 time steps respectively, so that the exponentially decaying grating strength is of the form

$$A(t) = A_0 \exp(-t/\tau_1),$$

and the growth curve, during this interval, follows the form given by

$$B(t) = B_0 [1 - \exp(-t/\tau_2)].$$

Between time step 1 to 100 in fig. 3, the pusher is stationary, and the resultant subtraction is shown as the solid curve. It is clear from this idealized model, that a time occurs when the output is reduced to zero (time step ≈ 15) and complete subtraction has been obtained. This situation however will not last for the whole of the cycle covered by this time-step range, due to the growth and decay dynamics; therefore the subtraction curve shows an imperfect subtraction for much of this range.

If however, we choose to either increase the time constants τ_1 and τ_2 , or equivalently, to increase the pushing frequency (for given values of τ_1 and τ_2), we would expect to see improved subtraction over essentially the complete cycle. Note that in both cases, the sequence above is reversed for the interval between time steps $t=101$ and 200. The subtraction

curve demonstrates a frequency doubling compared to the pushing frequency. For practical implementation of such a scheme, one must consider the temporal build up, and decay, of both these sequentially recorded gratings. If either the writing or erasure times are comparable with the applied periodic phase modulation, then any such subtraction is also dynamic, and ideal subtraction will therefore be compromised. Deliberate motion of the input object will also produce non-optimum subtraction, so that moving areas within an input field will be seen in the output.

Fig. 4 column (i) shows oscilloscope traces recorded on a storage scope of the phase conjugate output from the complementary gratings detected at the image plane by a photodiode. The intensities of beams I_1 , I_2 , and I_3 were 7.0 mW, 3.5 mW and 2 mW respectively. Curve (a) shows the output when no ac square voltage waveform was applied to the pusher, and therefore one grating is present only. Traces (b), (c), (d), (e), and (f) show the output from the

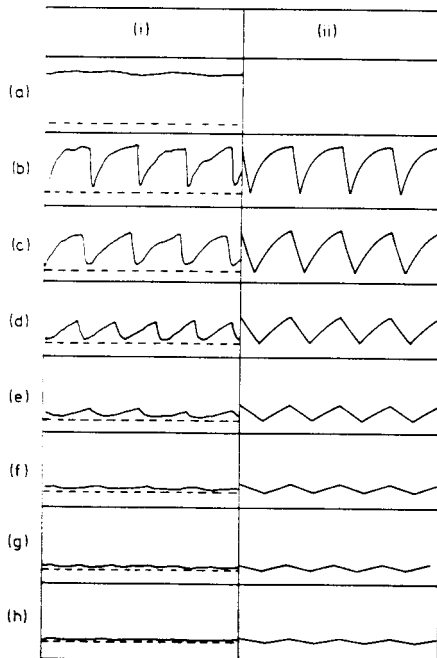


Fig. 4. Column (i): oscilloscope traces of the phase conjugate output. Column (ii): corresponding simulations for piezo-electric pusher frequencies of 1 Hz, (b), 2 Hz (c), 5 Hz (d), 10 Hz (e), 20 Hz (f), 30 Hz (g), and 40 Hz (h) respectively.

complimentary gratings for 1 Hz, 2 Hz, 5 Hz, 10 Hz, and 20 Hz respectively.

When the pusher was driven at a frequency of 30 Hz, output trace (g) shows almost perfect subtraction. Any further increase in pushing frequency would produce better subtraction but is less usable for motion detection, to be discussed below, due to the higher rate of phase modulation. Fig. 4 column (ii) shows results of a simulation based upon the model shown in fig. 3, at pushing frequencies corresponding to those used experimentally. It is clear from this simulation that experiment and modelling are in close agreement.

Fig. 5a shows the photograph of a resolution test chart whose phase replica was placed in the object plane to demonstrate velocity filtering. Fig. 5b shows the result of image subtraction when complementary gratings are recorded at a pushing frequency of 30 Hz, and at intensities described above.

Fig. 6 shows the results of dynamic image subtraction however in which several intensity features are observed: a sequence of such output images is shown in figs. 6a–6m. In all these figures, even though all parts of the test chart were moved with identical speeds, the subtraction process has isolated particular features within the general field of motion. Photograph 6a reveals only horizontal features within the object as vertical features were moving with too high a speed. This is clearly due to the limited response time of the BSO phase conjugate mirror under such conditions. In all cases the motion of the object was simple harmonic (pendulum-like behaviour). The displacement along the vertical axis was much smaller than along the horizontal axis, which gave rise to preferential observation of all horizontal features. In

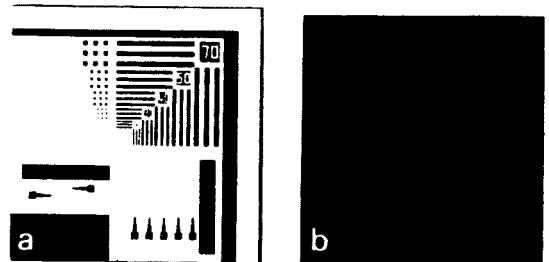


Fig. 5. (a) A photograph of a resolution test chart whose phase version was placed in the object plane. (b) The image subtraction under static condition.

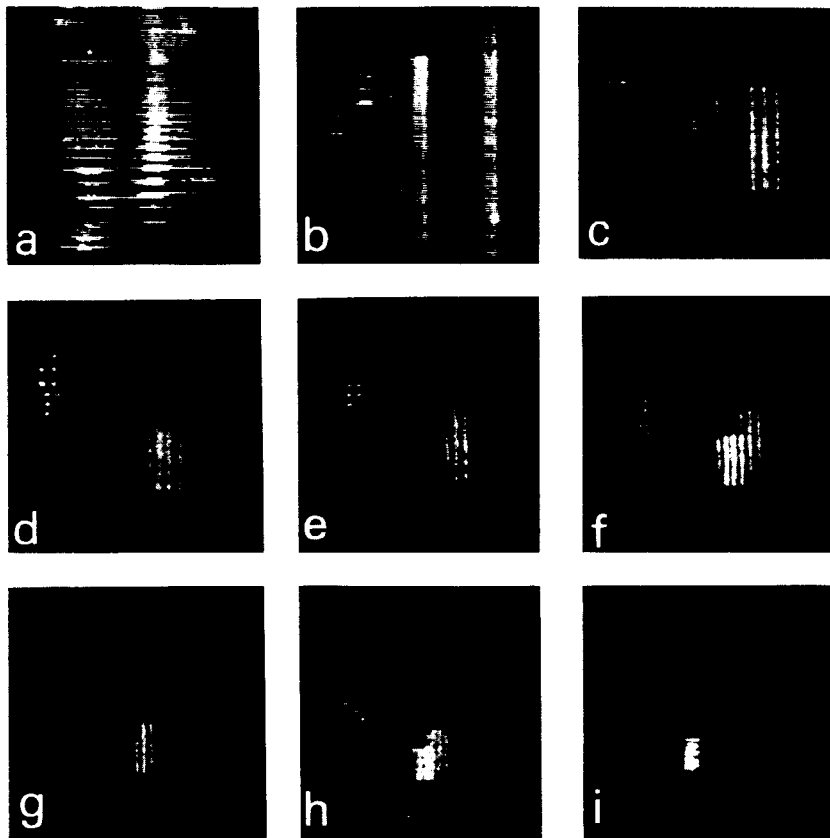


Fig. 6. Sequence of photographs showing velocity filtering detection of features of particular dimensions only observed at specific speeds.

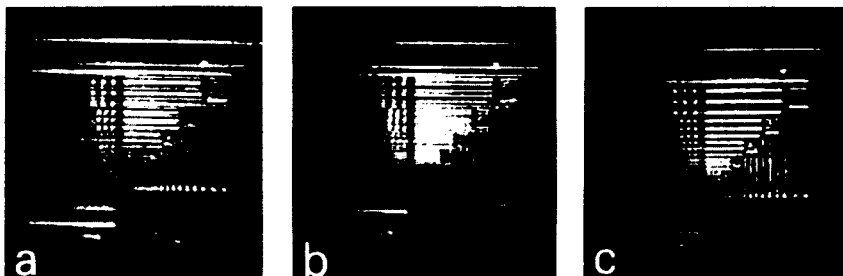


Fig. 7. Photographs showing different stages of motion detection when the object was subjected to damped simple harmonic motion in the vertical direction.

photograph 6b however, predominantly vertical features are observed, as the induced motion was much slower than that in 6a. Figs. 6c–6i show a sequence of outputs, representing specific times within the cyclic oscillatory motion for the same input phase object, but revealing the feature extraction aspects of

this velocity filtering technique. It is seen that for any specific velocity within the overall velocity range, only a specific dimensional feature is readily apparent. The feature sizes shown here vary from 70 μm width in fig. 6c, to the smallest features observable with the limited numerical aperture in our experi-

mental arrangement, of 20 μm . It can therefore be concluded that the observed features depend on a unique combination of size and velocity, which allows an accurate size estimate to be made, knowing the velocity, and vice versa.

A different aspect of velocity detection is shown in fig. 7 where the object was merely subjected to a fast, small amplitude damped simple harmonic, displacement in the vertical direction. Because, in this case, a repetitive continuous range of velocities is present, no discrimination occurs between respective feature sizes as was apparent in fig. 6. In this latter case therefore, a differentiation in time is pro-

duced and the small amplitude, high frequency motion does not discriminate against size.

The final aspect of this technique illustrates the implementation of a Fourier transform stage, in a similar manner to that of ref. [2], where directional motion detection was also reported, but now, with the added capability of identifying specific feature sizes. Fig. 8a shows the Fourier transform of subtraction achieved via complementary gratings. Fig. 8b shows higher order vertical Fourier components, corresponding to the appearance of horizontal detail in the output image as observed in fig. 6a for example. Figs. 8c–8f show a similar sequence to the results of fig. 6, where the benefit of the added Fourier stage are observed. In fig. 8e for example, the orders that appear are directly interpretable as distinct feature size within the output image plane.

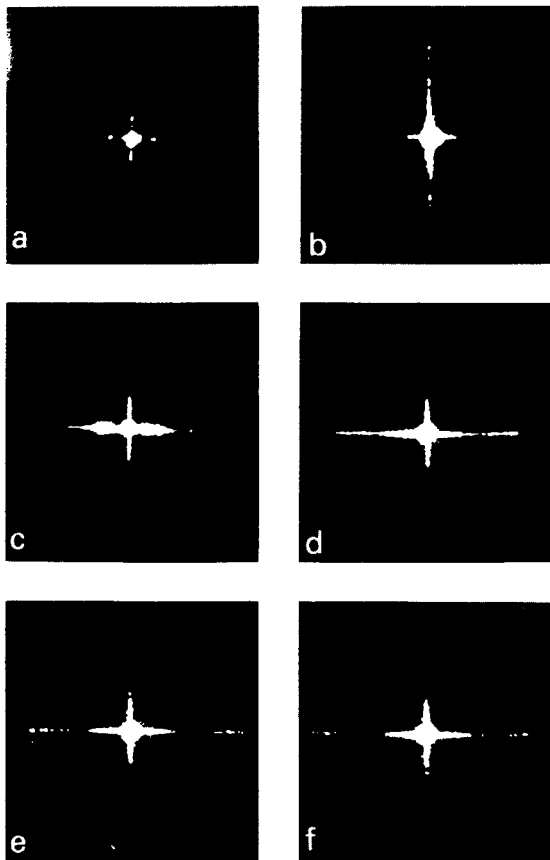


Fig. 8. Results of directional motion detection via a Fourier transformation stage. (a) Fourier transform of subtraction of a static resolution chart showing faint dc term only. (b) Appearance of vertical orders only due to horizontal features present in the output image. (c) shows no discrimination between horizontal and vertical orders at a lower speed. (d), (e), and (f) show a sequence of higher horizontal orders due to the lower speeds.

4. Conclusion

A technique for velocity filtering has been demonstrated. Our technique is based on complementary (multiplexed) grating formation in a single crystal of BSO, in a DFWM arrangement. Under static conditions no output is observed; however under induced motion, we observe a bright output image whose features depend on the particular speed. At speeds above and below this the output image is greatly reduced and experimental results are presented to verify this velocity filtering operation. Results are also presented for Fourier transform implementation.

Acknowledgements

We are grateful to the Government of Pakistan and Overseas Research Scheme for a studentship for G.H., and acknowledge research funding under SERC grant no. GR/F84256. We are also grateful to J. Khoury for earlier discussions concerning these ideas.

References

- [1] D.Z. Anderson, D.M. Liniger and J. Feinberg, *Optics Lett.* 12 (1987) 128.

- [2] J.A. Khoury, G. Hussain and R.W. Eason, *Optics Comm.* 71 (1989) 138.
- [3] M. Cronin-Golomb, A.M. Biernacki, C. Lin and H. Kong, *Optics Lett.* 12 (1987) 1029.
- [4] R.S. Cudney, R.M. Pierce and J. Feinberg, *Nature* 332 (1988) 424.
- [5] T. Aida, K. Takizawa and M. Okada, *Optics Lett.* 14 (1989) 835.
- [6] Y. Li, A. Kostrzewski, D.H. Kim and G. Eichmann, *Appl. Optics* 28 (1989) 4861.
- [7] P. Gunter and J.-P. Huignard, *Photorefractive materials and their applications. Topics in Applied Physics, Vols. 61 (1988), 62 (1989) (Springer, Berlin).*
- [8] J.P. Huignard, J.-P. Herriau and F. Micheron, *Ferroelectrics* 11 (1976) 393.
- [9] N.A. Vainos and R.W. Eason, *Optics Comm.* 62 (1987) 311.